



LUND UNIVERSITY

Sub-100-nm gate-length scaling of vertical InAs/InGaAs nanowire MOSFETs on Si

Kilpi, Olli Pekka; Svensson, Johannes; Wernersson, Lars Erik

Published in:
2017 IEEE International Electron Devices Meeting, IEDM 2017

DOI:
[10.1109/IEDM.2017.8268408](https://doi.org/10.1109/IEDM.2017.8268408)

2018

[Link to publication](#)

Citation for published version (APA):
Kilpi, O. P., Svensson, J., & Wernersson, L. E. (2018). Sub-100-nm gate-length scaling of vertical InAs/InGaAs nanowire MOSFETs on Si. In *2017 IEEE International Electron Devices Meeting, IEDM 2017* (Vol. Part F134366, pp. 17.3.1-17.3.4). IEEE - Institute of Electrical and Electronics Engineers Inc..
<https://doi.org/10.1109/IEDM.2017.8268408>

Total number of authors:
3

General rights

Unless other specific re-use rights are stated the following general rights apply:
Copyright and moral rights for the publications made accessible in the public portal are retained by the authors and/or other copyright owners and it is a condition of accessing publications that users recognise and abide by the legal requirements associated with these rights.

- Users may download and print one copy of any publication from the public portal for the purpose of private study or research.
- You may not further distribute the material or use it for any profit-making activity or commercial gain
- You may freely distribute the URL identifying the publication in the public portal

Read more about Creative commons licenses: <https://creativecommons.org/licenses/>

Take down policy

If you believe that this document breaches copyright please contact us providing details, and we will remove access to the work immediately and investigate your claim.

LUND UNIVERSITY

PO Box 117
221 00 Lund
+46 46-222 00 00

Sub-100-nm Gate-Length Scaling of Vertical InAs/InGaAs Nanowire MOSFETs on Si

Olli-Pekka Kilpi¹, Johannes Svensson¹, and Lars-Erik Wernersson¹

¹Department of Electrical and Information Technology, Lund University, Lund, Sweden, email: olli-pekka.kilpi@eit.lth.se

Abstract—We demonstrate a process to vary the gate-length of vertical MOSFETs on the same sample with high accuracy and high performance. Fabricated vertical InAs/InGaAs MOSFETs on Si have gate length ranging from 25 nm to 140 nm. The results shown are from single nanowire transistors as well as arrays with nanowires ranging from 80 to 500 nanowires. The devices show good yield and clear scaling trends. We demonstrate a device with $g_m = 2.4$ mS/ μ m and a device with $I_{on} = 407$ μ A/ μ m at $I_{off} = 100$ nA/ μ m and $V_{DD} = 0.5$ V, which both are record values for vertical MOSFETs. This is the first demonstration of vertical MOSFETs having gate-lengths comparable to the state-of-the-art lateral III-V MOSFETs.

I. INTRODUCTION

Vertical MOSFETs are considered to extend the transistor scaling at the extremely scaled nodes. Technology comparison have shown, that the vertical structure offers improved performance at the extremely scaled nodes as more space is available for contacts and spacers, when compared to FinFETs and laterally stacked gate-all-around (GAA) MOSFETs [1]. Vertical nanowire structure further allows integration of high-mobility materials on Si due to the possibility to relax stress originating from the lattice mismatch. Several demonstration of vertical MOSFETs have been published [2 - 7], however so far vertical MOSFETs with scaled gate-lengths have not been demonstrated. It is necessary to scale the gate-length, even though the gate-length in vertical MOSFETs is decoupled from the footprint, in order to improve the performance.

In this work, we demonstrate vertical InAs/InGaAs heterostructure MOSFETs on Si with the gate length (L_G) down to 25 nm. The gate length is scaled from 25 nm to 140 nm showing clear scaling trends in all transistor metrics. By L_G scaling and introducing a different drain contact metal, we manage to achieve $g_m = 2.4$ mS/ μ m and $I_{on} = 407$ μ A/ μ m at $I_{off} = 100$ nA/ μ m and $V_{DD} = 0.5$ V, which both are the highest values reported on vertical MOSFETs.

II. DEVICE FABRICATION

Illustration of the device fabrication and scanning electron micrographs (SEM) of the devices are shown in figures 1 and 2, respectively. The device fabrication is started by growing 300-nm-thick InAs source contact by metal-organic-vapor-phase-deposition (MOCVD) on Si and electron beam lithography (EBL) defining gold particles on top of the InAs layer. The nanowires are grown by using gold particle catalytic vapor-liquid-solid (VLS) growth in MOCVD. For the growth, two different gold particle sizes were used (diameter 28 nm and

32 nm). The nanowire structure is similar to earlier published results [2]. The growth is started by growing 100 nm unintentionally doped InAs, which is followed by 100-nm-long unintentionally doped grading from InAs to In_{0.5}Ga_{0.5}As. The nanowire growth is finalized, by growing 300-nm-long highly doped In_{0.5}Ga_{0.5}As, which also overgrows the unintentionally doped part forming a core shell structure. The thickness of the unintentionally doped core is approximately 30 nm and the thickness of the whole nanowire is approximately 50 nm. For the MOSFET fabrication single nanowires as well as double-row arrays (nanowire spacing 200 nm) ranging from 80 to 500 nanowires were used.

The fabrication of the transistor is started by fabricating the drain contact. The location of the drain contact can be controlled by the thickness of the sacrificial hydrogen silsesquioxane (HSQ) layer, which thickness can be altered within the same sample by changing the EBL dose [7]. The drain fabrication is started by spin-coating, EBL defining, and developing sacrificial HSQ layer in TMAH (25%). The process is followed by sputtering 20-nm-thick Mo layer and ALD depositing 3-nm-thick TiN. The metals are anisotropically etched and the HSQ removed, therefore leaving metal only on the sidewalls of the nanowires. The processing is followed by fabricating the HSQ bottom spacer. The thickness of the HSQ spacer can be, as well, controlled by the EBL dose, therefore allowing good spacer control, which makes possible the fabrication of gate-lengths as small as 25 nm. In this work, the bottom HSQ was 140-nm-thick and the position of the drain contact was increased, so that the gate-length was varied from 25 to 140 nm.

After the top part of the nanowire is covered by the drain metal and the bottom part by the HSQ spacer, the gate region is locally etched using digital etching. In other words, the gate region is oxidized in ozone and the formed native oxide removed by HCl. This etching is repeated until the highly doped shell is removed. A bilayer Al₂O₃/HfO₂ (ALD cycles 10/37) was deposited and followed by deposition of 50-nm-thick W gate metal. The device is completed by etching the excess gate metal, depositing organic (S1813) second spacer, and fabricating contacts.

III. RESULTS

Transfer and output characteristics of the device with 120 nanowires, diameter of 27 nm and $L_G = 75$ nm are shown in figures 3 and 4, respectively. The device has $g_m = 1.90$ mS/ μ m (normalized to the circumference) and $SS = 86$ mV/dec. Q-value (g_m/SS) = 22 and $I_{on} = 407$ μ A/ μ m at $I_{off} = 100$ nA/ μ m and $V_{DD} = 0.5$ V, which are the highest reported on vertical

MOSFETs. The device has the SS of 81 mV/dec and 86 mV/dec at 50 mV and 500 mV, respectively, as shown in figure 5. The device shows good electrostatics by having $DIBL = 80$ mV/V at $1 \mu\text{A}/\mu\text{m}$ and reasonably low access resistance by having $R_{\text{on}} = 450 \Omega\mu\text{m}$.

Transfer and output characteristics of the single nanowire transistor with diameter of 37 nm and $L_G = 45$ nm are shown in figures 6 and 7. The device shows record high $g_m = 2.4$ mS/ μm in vertical MOSFETs and low $R_{\text{on}} = 340 \Omega\mu\text{m}$. However, due to the relatively large diameter and shorter gate-length, the device cannot be fully turned off, which cause $DIBL = 290$ mV/V and $SS = 138$ mV/dec.

In figure 8, the transfer characteristics of the device with 80 nanowires, diameter 28 nm and $L_G = 75$ nm is shown. The device is biased in two different configurations, by having the drain at the top (bottom grounded) and by having the drain at bottom (top grounded). The device shows clear asymmetry by having one order of magnitude lower off-current and higher g_m in the bottom ground configuration. The device also shows asymmetry in subthreshold behavior by having $SS = 91$ mV/dec in bottom ground configuration and $SS = 116$ mV/dec in top ground configuration. These differences are attributed to the location of the InGaAs, which is on the drain side on the bottom ground configuration and at the source side on the top ground configuration. The introduction of Ga reduces the probability for gate-to-drain tunneling. In addition, the contacts have asymmetry, which most likely slightly decreases performance in top ground configuration by having larger contact resistance on the source side.

Figure 9-14 show different transistor metrics versus the gate length. In figure 9, g_m versus L_G is shown. g_m clearly increases, when the gate length is scaled, as expected. However, below $L_G = 45$ nm, g_m starts decreasing. This decrease is attribute to short channel effects, as well as a possible problem to fully gate the unintentionally doped channel. Figure 10 shows similar scaling of I_{off} , which behaves as expected. I_{off} seems to stabilize below 100 nA/ μm at gate-lengths 75 nm and larger. At smaller gate-lengths devices of this diameter cannot be fully turned off having I_{off} well above 100 nA/ μm . The heterojunction is expected to be at approximately $L_G = 50$ nm, which together with longer gate-length explains the steep drop of the I_{off} at $L_G > 50$ nm.

In figure 11 R_{on} versus L_G is shown. In the figure, only devices with the seed particle of 28 nm are shown, although devices with larger seed particle have slightly lower R_{on} . Dashed line shows a linear fit, where devices with $L_G = 25$ nm are excluded, as the R_{on} seems to flatten at lower gate lengths. The increased resistance at shorter gate lengths could be attributed to ungated regions without channel doping. Extrapolating the linear fit, an access resistance of $212 \Omega\mu\text{m}$

can be determined. The access resistance is largely reduced from previously reported values, which could be attributed to the use of Mo top metal.

Figure 12 and 13 show SS and V_T versus gate-length. Both metrics show the expected scaling trend. SS increases at the shortest gate lengths and V_T decreases due to short channel effects. In figure 14, maximum intrinsic gain (g_m/g_d) versus L_G is shown. g_m/g_d peaks at $L_G = 75$ nm, as we are able to maintain good g_d at low gate-lengths due to gate-all-around structure.

Figure 15 shows device scaling by plotting g_m versus the number of nanowires in the array. g_m increases linearly with increasing number of nanowires demonstrating good yield and process control. The devices with $50 \text{ nm} < L_G < 100 \text{ nm}$ show the highest g_m . In figure 16, our best devices are benchmarked against the state-of-the art vertical devices. Our devices show clear improvement in terms of g_m/SS , showing the highest Q-value = 22. In figure 17, our best devices are benchmarked versus state-of-the-art III-V MOSFETs. Our devices clearly have higher I_{on} at $I_{\text{off}} = 100$ nA/ μm and $V_{\text{DD}} = 0.5$ V than state-of-the-art vertical MOSFETs. However, state-of-the-art lateral InGaAs MOSFETs still show higher I_{on} than the presently studied transistors.

IV. CONCLUSIONS

We have developed a process to vary the gate length of the vertical MOSFETs on the same sample and fabricate devices with gate-length as low as 25 nm. We demonstrate vertical InAs/InGaAs nanowire MOSFETs on Si with gate-length varying from 25 nm to 140 nm. The devices show clear scaling trends. In addition, the devices have the highest $g_m = 2.4$ mS/ μm and $I_{\text{on}} = 407 \mu\text{A}/\mu\text{m}$ at $I_{\text{off}} = 100$ nA/ μm and $V_{\text{DD}} = 0.5$ V reported for vertical MOSFETs.

ACKNOWLEDGMENT

This work was supported in part by the Swedish Research Council, in part by the Knut and Alice Wallenberg Foundation, in part by the Swedish Foundation for Strategic Research and in part by the European Union H2020 program INSIGHT (Grant Agreement No. 688784)

REFERENCES

- [1] D. Yakimets, et al., TED, vol. 62, pp. 1433, (2015).
- [2] O.-P. Kilpi, et al, VLSI, (2017)
- [3] M. Berg, et al, IEDM, pp. 31.2.1-31.2.4, (2015)
- [4] X. Zhao, et al., IEDM, pp. 28.4.1-28.4.4, (2013)
- [5] S. Ramesh, et al., VLSI, (2016)
- [6] X. Zhao, et al., TED, vol. 64, pp. 2161, (2017)
- [7] E. Memisevic, et al., J. Vac. Sci. Technol. vol. 32, pp. 051211 (2014)
- [8] C. B. Zota, et al., IEDM, pp. 3.2.1-3.2.4 (2016)
- [9] S. Lee, et al, VLSI, (2014)

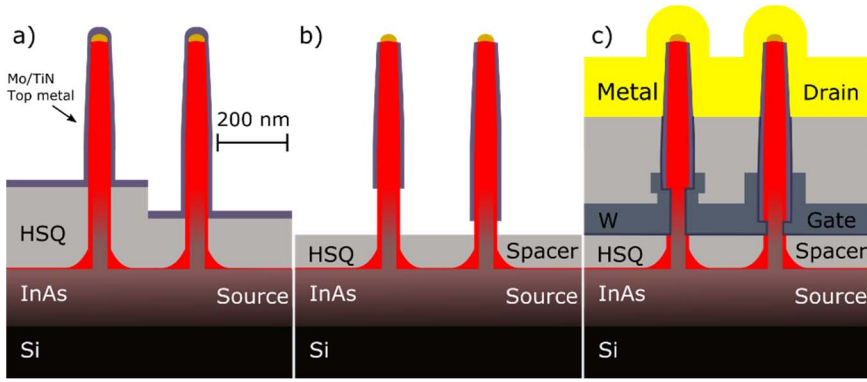


Fig. 1. Illustration of the process after top metal deposition (a), first spacer deposition (b) and final contacts (c). The gate-length can be controlled by controlling EBL dose in the top metal and bottom spacer fabrication.

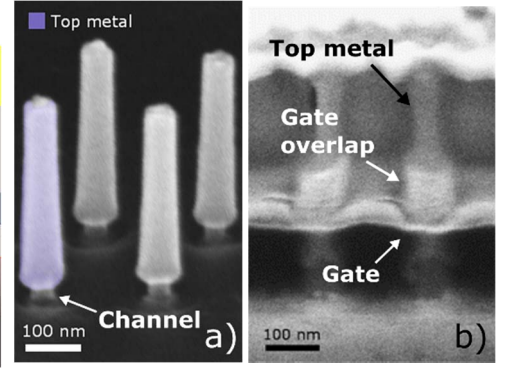


Fig. 2. SEM of the device with $L_G = 25$ nm after high- κ deposition (a). Completed device (b) has a large gate-drain overlap due to having different gate-lengths on the same sample.

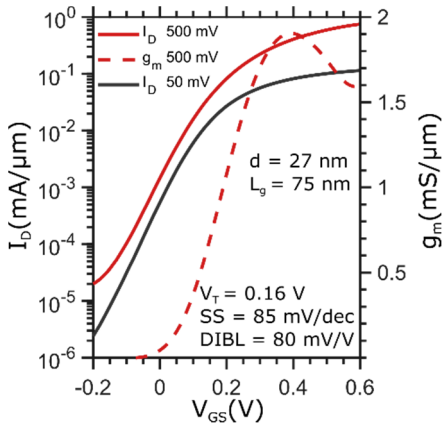


Fig. 3. Transfer characteristics of the array with 120 nanowires, diameter 27 nm and $L_G = 75$ nm.

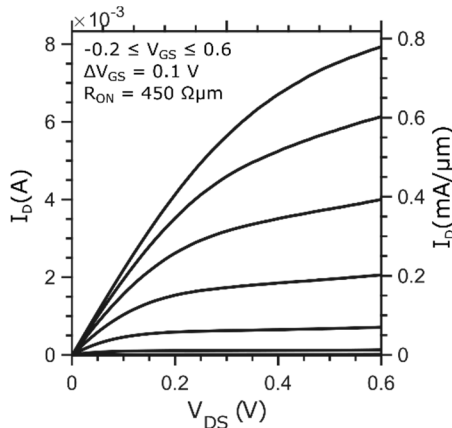


Fig. 4. Output characteristics of the array with 120 nanowires, diameter 27 nm and $L_G = 75$ nm.

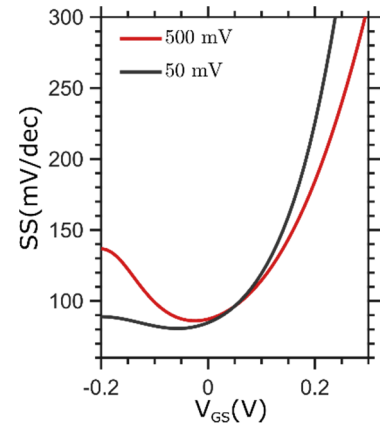


Fig. 5. Subthreshold swing of the array with 120 nanowires, diameter 27 nm and $L_G = 75$ nm.

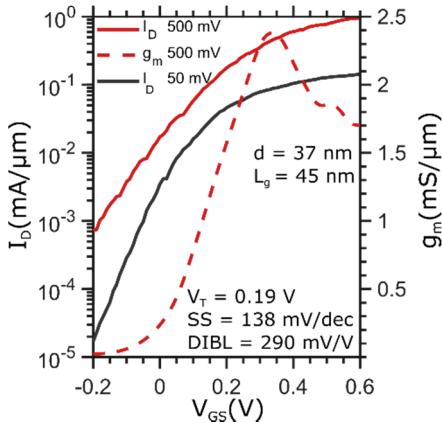


Fig. 6. Transfer characteristics of single nanowire transistor with diameter 37 nm and $L_G = 45$ nm.

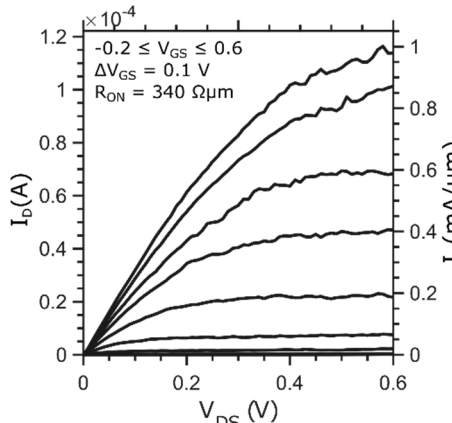


Fig. 7. Output characteristics of single nanowire transistor with diameter 37 nm and $L_G = 45$ nm.

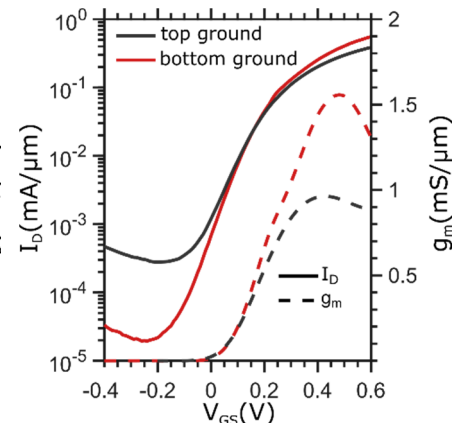


Fig. 8. Transfer characteristics of the array with 80 nanowires, diameter 27 nm and $L_G = 75$ nm. Measured in two different configurations (bottom and top ground).

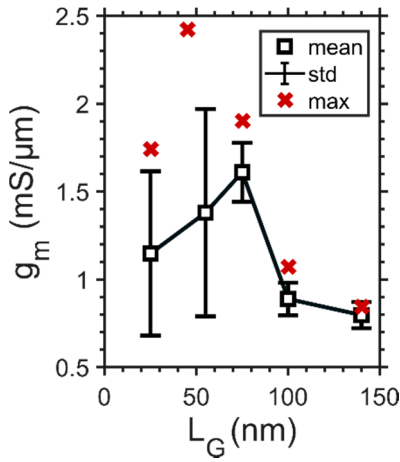


Fig. 9. Mean and peak $g_{m,\text{max}}$ of the devices with different L_G .

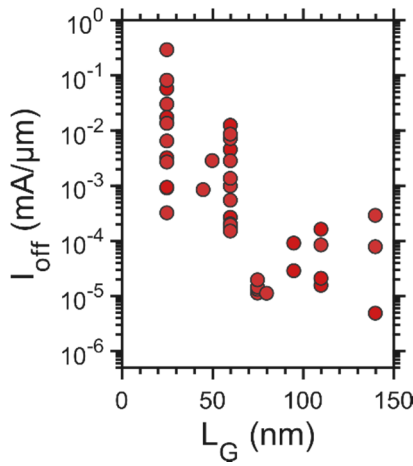


Fig. 10. I_{off} of the devices with different L_G .

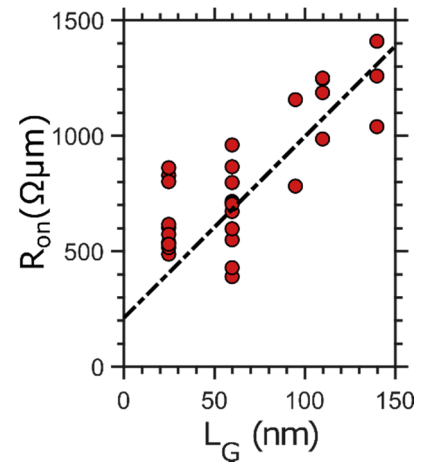


Fig. 11. R_{on} of the devices with different L_G . Extrapolation gives an access resistance of 212 $\Omega\mu\text{m}$.

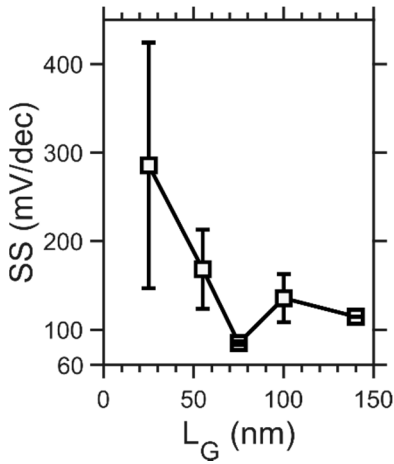


Fig. 12. Mean and peak SS_{min} of the devices with different L_G .

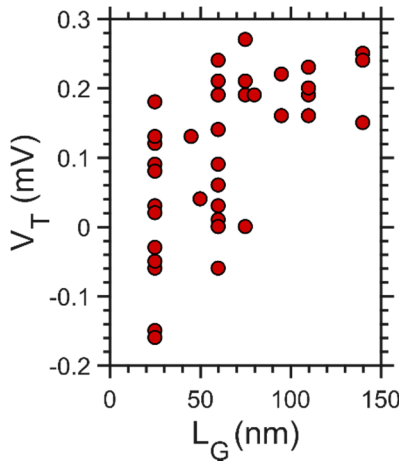


Fig. 13. V_T of the devices with different L_G .

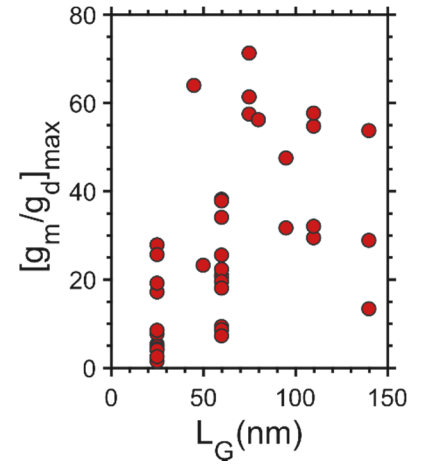


Fig. 14. Maximum g_m/g_d with different L_G .

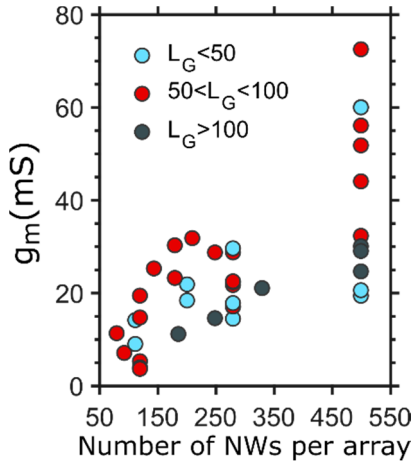


Fig. 15. Unnormalized g_m versus number of nanowires in the transistor.

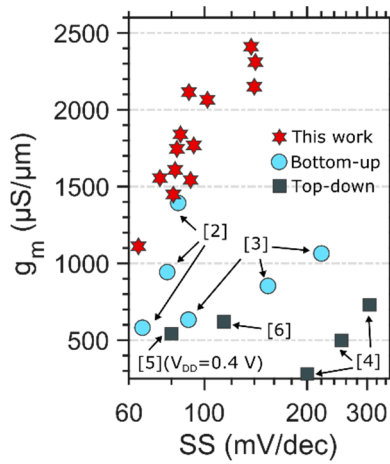


Fig. 16. The devices benchmarked versus the state-of-the-art vertical III-V MOSFETs.

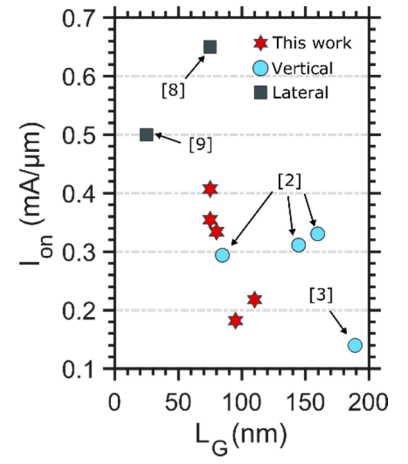


Fig. 17. The devices benchmarked versus lateral and vertical III-V MOSFETs.